NEAR-COLORLESS HPHT SYNTHETIC DIAMONDS FROM AOTC GROUP

Ulrika F.S. D'Haenens-Johansson, Kyaw Soe Moe, Paul Johnson, Shun Yan Wong, Ren Lu, and Wuyi Wang

The gemological and spectroscopic properties of 52 colorless to fancy light-colored HPHT synthetic diamonds (40 of them colorless or near-colorless) produced by AOTC using either toroid- or BARS-press technologies were characterized. In addition to achieving excellent color grades, these commercially available faceted synthetics had a weight range of 0.05 to 0.80 ct, and possessed IF to I_2 clarity. Their synthetic origin may be difficult to determine with standard gemological techniques alone, but they were conclusively identified using advanced testing methods, including photoluminescence, FTIR spectroscopy, and fluorescence imaging. Inclusions in two samples, grown by different press types, were studied using LA-ICP-MS. The trace-elemental analysis results indicated that the inclusions formed by the trapping of the solvent/catalyst melt during synthesis. Analysis of the combined multi-technique data provided insight into the identities of the solvents, catalysts, and nitrogen getters possibly used to grow high-quality HPHT synthetic diamonds.

In the gem trade, natural diamonds with D to Z color are significantly more abundant than their fancy-color counterparts. The opposite is true for gem-quality synthetic diamonds, where near-colorless specimens are more challenging to produce. Most synthetic diamonds used for jewelry are produced by either high-pressure, high-temperature (HPHT) or chemical vapor deposition (CVD) techniques. Advances in CVD technologies, as well as an improved understanding of the growth processes, led to the introduction of near-colorless CVD synthetic diamonds around the middle of the last decade (Wang et al., 2007) by companies such as Apollo Diamond Inc. (sold in 2011 to Scio Diamond Technology). More recently, the near-colorless CVD synthetic diamond market has expanded with the large-scale production from Gemesis Corporation, which reportedly applies color-enhancing post-growth treatments to its as-grown material (Wang et al., 2012a). CVD synthetics have garnered significant publicity based on instances where samples have been submitted to gemological laboratories without disclosure of their unnatural origin (Even-Zohar, 2012).

Although well known in the colored diamond market, HPHT-grown synthetics have not played a significant role in the mainstream colorless diamond trade. Most colorless to near-colorless faceted HPHT synthetic specimens have been grown solely for research purposes by companies such as General Electric (Crowningshield, 1971; Koivula and Fryer, 1984; Shigley et al., 1993), De Beers (Rooney et al., 1993; Burns et al., 1999), and Sumitomo Electric Industries (Shigley et al., 1997; Sumiya and Satoh, 1996; Sumiya et al., 2002). Near-colorless HPHT synthetics have also been marketed within the gem trade, in notably limited quantities, by Chatham Created Diamonds, Starcorp, and Advanced Optical Technology Corporation (AOTC), now trading as AOTC Group, B.V. (see Koivula et al., 1994; Shigley et al., 1997; Deljanin et al., 2006; D'Haenens-Johansson et al., 2012).

In 2012, three near-colorless and three faintly colored HPHT-grown AOTC synthetic diamonds were submitted to GIA's New York laboratory for grading services. These samples, in addition to 24 colorless, near-colorless, faintly colored, and lightly colored faceted HPHT synthetics on loan from AOTC, were studied and briefly reported on in *Gems & Gemology* (D'Haenens-Johansson et al., 2012). GIA subse-

See end of article for About the Authors and Acknowledgments.
GEMS & GEMOLOGY, Vol. 50, No. 1, pp. 30–45,
http://dx.doi.org/10.5741/GEMS.50.1.30.

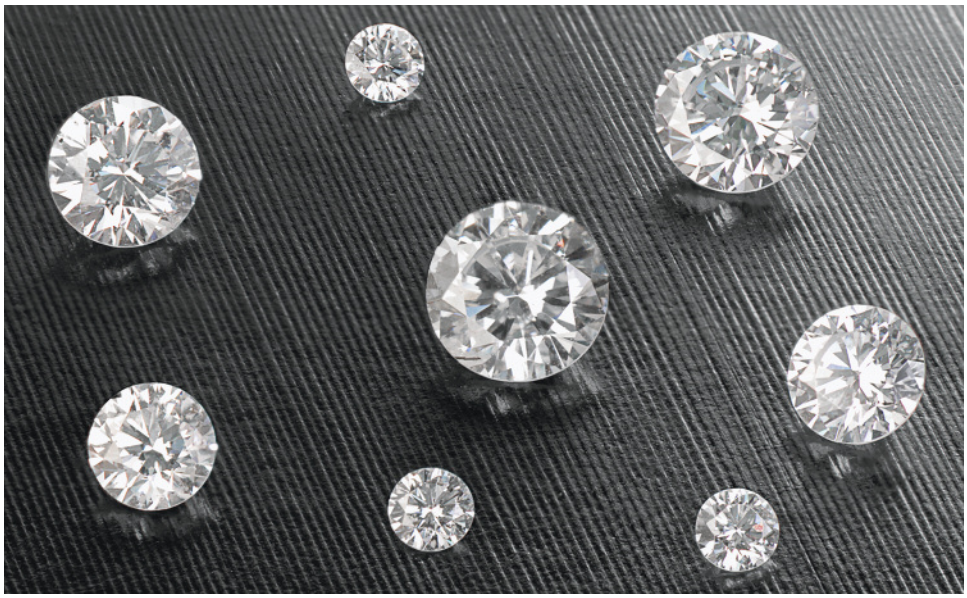

Figure 1. This photograph shows eight of the 52 faceted HPHT synthetic diamonds obtained from AOTC Group, ranging from 0.05 to 0.57 ct. Of the total suite of samples examined, 40 were graded as colorless to near-colorless, a remarkably good color range for HPHT synthetic diamonds, which are commonly produced in fancy colors. Photo by Josh Balduf.

quently obtained another 22 samples from AOTC, including 10 melee-sized synthetic diamonds. This article will present the results of the investigation using gemological and spectroscopic techniques on the full suite of 52 AOTC synthetic diamonds (selected samples are shown in figure 1). Although their properties are comparable to those of top-quality natural diamonds, it is still possible to identify them as HPHT synthetics.

AOTC is a privately owned synthetic gem diamond company headquartered in the Netherlands, with offices in Germany, Switzerland, Canada, and the United States. AOTC's faceted HPHT synthetic diamonds can be purchased through their company website (by members of the jewelry trade only) or through D.NEA, an online retail operation that sells their synthetics, both loose and in jewelry pieces. The products retail with full disclosure of their laboratory origin, and samples weighing more than 0.30 ct bear the laser inscription "AOTC-created" (D.NEA, 2014a). Although most of its production is focused on fancy-color yellow and blue HPHT synthetics, AOTC also grows near-colorless (labeled "white") synthetic diamonds using BARS- and toroid-press technologies. The company's yellow HPHT synthetic diamonds,are sold in sizes up to 3 ct; however, the blue and "white" synthetics weigh no more than 1.5 ct (D.NEA, 2014b). Since these products are only available in faceted form, the as-grown "rough" specimens are considerably larger. D.NEA (2014c) reports selling its "white" synthetic diamonds at prices "15–40% less than comparable mined diamonds." Currently, AOTC is the dominant producer of near-colorless HPHT synthetic diamonds for the gem trade.

REVIEW OF HPHT SYNTHESIS OF DIAMOND

Diamond synthesis by HPHT methods was first carried out by the Swedish company ASEA in 1953, but the synthetic diamond era truly began a year later, when scientists at General Electric (GE) independently reported the growth of diamond using this technique (Bundy et al., 1955). Prior to GE's success, diamond and graphite had already been established as carbon *allotropes* (i.e., consisting of different structural configurations of the same element). It was originally thought that applying high temperatures and pressures to graphite, to some extent mimicking the growth conditions of natural diamond, would yield synthetic diamond, but this proved unsuccessful.

Through research, the process evolved into the temperature-gradient HPHT method. In this method (Bovenkerk et al., 1959), the HPHT capsule is filled with the carbon source material (typically graphite), a diamond "seed," and a solvent/catalyst (usually a group VIII element such as iron or its alloys). The use of a solvent/catalyst lowers the temperature and pressure conditions necessary for successful diamond growth. Alloys such as Fe-Ni and Fe-Co are widely used because of their lower melting points (and thus lower pressures required). The system's pressure and temperature are increased so that the solvent/catalyst melts; the resulting diamond is the thermodynamically stable form of carbon. The conditions vary depending on the size, quality, and type of diamond synthesized, but the pressures and temperatures ap-

plied are usually in the ranges of 5–6 GPa and 1300–1600°C, respectively (Burns et al., 1999). A temperature gradient (i.e., difference in temperature) is carefully produced, such that the carbon source material is located in a hotter region than the diamond seed. The source material dissolves, and the carbon atoms are transported toward the cooler region, where the dissolved carbon becomes supersaturated in the solvent, crystallizing on the diamond seed and forming new diamond. Four main types of presses are used to grow diamond by this method: belt, BARS (based on a split-sphere concept), cubic, and toroid presses (see e.g. Strong and Chrenko, 1971; Strong, 1989; Bundy et al., 1973; Shigley et al., 1993; Khvostantsev et al., 2004).

Chemical impurities and macroscopic inclusions from the solvent/catalyst are easily incorporated into the growing diamond. Nitrogen contamination may originate from the solvent/catalyst, the carbon source, or the gas found in the empty spaces or pores of the HPHT capsule. The nitrogen impurities enter the structure of the nascent diamond as substitutional atoms, resulting in yellow type Ib material with nitrogen concentrations in the range of 100 to 300 atomic parts per million (Burns et al., 1999). Most of the HPHT synthetic diamonds produced worldwide are type Ib. Synthesis time and temperature conditions permitting, the isolated nitrogen atoms may also aggregate into pairs, forming A-centers and resulting in mixed type Ib/IaA synthetic diamonds (Chrenko et al., 1971 and 1977).

To reduce impurity concentrations and create near-colorless type IIa or weak type IIb diamonds, it is insufficient to merely use higher-purity solvents/catalysts and carbon sources. It is also necessary to introduce a *nitrogen getter*, usually an element with a strong affinity for nitrogen, such as aluminum (Al), titanium (Ti), zirconium (Zr), or hafnium (Hf). A significant amount of the nitrogen in the growth capsule will thus be "trapped," forming nitrides. Nevertheless, the introduction of the nitrogen getter may promote the uptake of solvent/catalyst inclusions, due to the reduced solubility of the carbon in the solvent/catalyst or changes in the diffusion of the carbon. To minimize this effect, it may be advantageous to slow the growth rate by adjusting the temperature. The nitrogen getter may also react with the carbon to form carbides that can be incorporated in the HPHT synthetic diamond, reducing its clarity. A suitable element (such as copper) may be further added to decompose these carbides (see Strong and Chrenko, 1971; Burns et al., 1990; Sumiya and Satoh, 1996; Sumiyu et al., 1996).

Type IIb synthetic diamonds with colors ranging from pale blue to opaque blue-black can also be created by doping the material with boron. To do this in a controlled manner, the nitrogen concentration is simultaneously reduced by adding nitrogen getters. The blue color arises from uncompensated boron, or the amount of boron in excess of the substitutional nitrogen concentration at the atomic ppm level (Burns et al., 1999).

Fancy-color HPHT synthetic diamond products, available to the gem trade since the early 1990s, have been extensively characterized (e.g., Shigley et al., 1993b, 2002). The complex mixture of ingredients in the growth capsule, combined with the need for sensitive control of temperature and pressure for extended periods of time, has made near-colorless HPHT diamond synthesis expensive and time consuming. Consequently, fewer near-colorless samples are available for study (Koivula et al., 1994; Shigley et al., 1997; Deljanin et al., 2006; D'Haenens-Johansson et al., 2012). AOTC indicates it can take more than two weeks to grow a synthetic "white" crystal that can be cut into a 1 ct synthetic diamond (D.NEA, 2014b). By comparison, AOTC states that growth periods for yellow and blue HPHT synthetic diamonds are 5–6 days and 7–10 days, respectively (D.NEA, 2014d,e). There is no post-growth treatment known to reduce color saturation in near-colorless HPHT synthetic diamonds, and AOTC claims to sell its "white" products in the as-grown state (D.NEA, 2014b). Although near-colorless HPHT synthetic diamond manufacturing for gem applications did not become commercially viable until recently, Sumitomo Electric Industries launched its Sumicrystal type IIa HPHT synthetic product in 1996. The company has reported the synthesis of diamonds as large as 8 ct for industrial applications (Sumiya and Satoh, 1996; Sumiya et al., 2002, 2005).

MATERIALS AND METHODS

All 52 of the faceted HPHT synthetic diamonds were round brilliants, ranging from 0.05 to 0.80 ct. Excluding the 10 melee-sized samples (all measuring 0.05 ct), the average weight was 0.37 ct. According to AOTC, 40 of the samples were grown using BARS presses, while the remaining 12 were created in toroid presses. Color and clarity grades were determined using the standard GIA grading systems for D to Z and fancy-color diamonds. Inclusions were investigated using a standard gemological binocular microscope system, as well as a Nikon SMZ1500 microscope with darkfield and fiber-optic illumination. The samples were also

examined under magnification between two crossed polarizing filters to detect anomalous birefringence (usually caused by strain). The color and clarity grades given in this article are for research purposes only. GIA's standard practice for synthetic diamond grading reports is to provide a color and clarity grade range.

Electrical conductivity was tested using a GIA electroconductometer, and magnetic properties were evaluated by suspending the sample from a thin thread and checking for motion when a strong magnet was brought toward it (Koivula and Fryer, 1984).

The samples' fluorescence and phosphorescence behavior to short- (254 nm) and long-wave (365 nm) ultraviolet light was investigated using a standard four-watt combination gemological testing lamp in a dark room. Additionally, fluorescence and phosphorescence images (5.0 second exposure and 0.1 second delay) were recorded using a DTC DiamondView instrument (< 230 nm excitation). Room-temperature phosphorescence spectra were collected using an Ocean Optics HR4000 spectrometer coupled with an Avantes-DH-S deuterium-halogen light source (215–2500 nm), as described by Eaton-Magaña et al. (2007, 2008). The experiment consisted of illuminating the sample for 20 seconds, switching off the light, and collecting phosphorescence spectra (1 second integration time) for a period of 120–180 seconds.

Room-temperature infrared absorption spectra were collected over the 6000–400 cm^{-1} range, at a resolution of 1 cm^{-1}, using a Thermo Nicolet Nexus 6700 FTIR spectrometer equipped with KBr and quartz beam splitters and a DRIFT (diffuse-reflectance infrared Fourier transform) unit. The system was purged with nitrogen gas to reduce absorption features from atmospheric water and carbon dioxide. IR spectra were normalized using the method of Palik (1985) to allow for calculation of defect concentrations.

Photoluminescence (PL) spectra were collected using a Renishaw InVia Raman confocal microspectrometer equipped with four laser systems, producing six excitation wavelengths: 324.8, 457.0, 488.0, 514.5, 632.8, and 830.0 nm. Samples were immersed in liquid nitrogen in a specially designed double-layer bath (patent pending) to maintain temperature at 77K (–196°C). Additional PL data were acquired using a Horiba XploRA Raman confocal microspectrometer with a 532.0 nm laser.

Trace-element analysis was conducted on surface-reaching inclusions in two samples, B0124 and T0130 (BARS- and toroid-press grown, respectively), using a ThermoFisher X-Series II laser ablation–inductively coupled plasma–mass spectrometer (LA-ICP-MS) equipped with a 213 nm laser ablation system. NIST SRM 610 and 612 glass standards were used for internal calibration. The system was run with a 7 Hz repetition rate and 16.09 J/cm^2 fluence. Spot sizes of 25 μm (B0124) or 30 μm (T0130) were chosen to ensure that only the inclusion material was sampled. The inclusions in B0124 and T0130 were laser-ablated for 45 and 30 seconds, respectively.

RESULTS

Color. As shown in table 1, most of the samples were graded as colorless in the D–F range (33%) or near-colorless in the G–J range (44%). Notably, the largest specimen (B0141, weighing 0.80 ct) had an impressive G color grade. The remaining samples displayed enough blue, green, or yellow-green coloration to be graded on the fancy color scale, with the strongest color saturation resulting in a Fancy Light blue grade. The color distribution in the latter samples was unusually even, without the zoning frequently observed in HPHT synthetics.

In Brief

- The 52 faceted colorless and near-colorless HPHT synthetic diamonds from AOTC studied in this report ranged in size from 0.05 to 0.80 ct, with 77% achieving colorless or near-colorless grades. Clarities ranged from IF to I_2.
- The HPHT synthetics were grown using BARS- and toroid-press technologies. PL and FTIR absorption spectroscopy, combined with trace element analysis of inclusions using LA-ICP-MS, suggest that different solvent/catalyst melts may be used during their synthesis.
- Although visual inspection may be insufficient to recognize their laboratory-grown origin, these samples could be positively identified as HPHT synthetic diamonds using PL spectroscopy and DiamondView fluorescence imaging.

Microscopy. The clarity of the suite ranged from IF to I_2, with no correlation between color and clarity grades (table 1). The melee-sized samples (B0152–B0162) had good clarity overall, with most receiving grades of VVS_2 or higher, including two IF samples. The poorer clarities resulted from elongated solvent/catalyst inclusions, which were opaque or metallic in appearance (figures 2 and 3), or from feathers. The results imply that samples grown using toroid presses are more likely to have distinct inclusions under 10× magnification, as nine of the 12 sam-

TABLE 1. Gemological properties and calculated bulk concentrations of neutral boron ($[B^0]$) impurities for HPHT synthetic diamonds from AOTC.[a]

Sample	Growth apparatus	Weight (ct)	Color	Clarity	Magnetic	Electrically conductive	$[B^0]$ bulk concentration (ppb)
B0117	BARS	0.22	Faint blue	VS_2	No	Yes	38 ± 5
B0118	BARS	0.34	F	VVS_2	No	No	-
B0119	BARS	0.28	F	VS_1	No	No	8 ± 1
B0120	BARS	0.30	Fancy Light blue	VS_2	Yes	Yes	216 ± 30
B0121	BARS	0.26	F	VS_2	Yes	No	3.2 ± 0.5
B0122	BARS	0.38	Very Light blue	SI_2	Yes	No	62 ± 9
B0123	BARS	0.39	H	I_1	No	Yes	21 ± 3
B0124	BARS	0.41	G	VS_2	Yes	No	7 ± 1
B0125	BARS	0.42	H	SI_1	Yes	Yes	47 ± 7
B0126	BARS	0.45	Very Light blue	SI_1	Yes	Yes	57 ± 9
B0127	BARS	0.54	J	VS_1	No	No	4.7 ± 0.7
B0128	BARS	0.57	J	VVS_1	No	No	12 ± 2
T0129	Toroid	0.20	H	I_1	No	No	-
T0130	Toroid	0.33	H	I_2	Yes	No	-
T0131	Toroid	0.32	I	I_2	Yes	No	-
T0132	Toroid	0.32	G	I_2	Yes	No	-
T0133	Toroid	0.21	H	VS_2	No	No	-
T0134	Toroid	0.21	I	VVS_1	No	No	-
T0135	Toroid	0.23	I	VVS_1	No	No	-
T0136	Toroid	0.23	F	I_1	Yes	No	-
T0137	Toroid	0.25	G	I_2	Yes	No	-
T0138	Toroid	0.25	F	I_2	Yes	No	-
T0139	Toroid	0.25	G	I_1	Yes	No	N/A
T0140	Toroid	0.27	J	I_1	Yes	No	-
B0141	BARS	0.80	G	VVS_1	N/A	N/A	49 ± 7
B0142	BARS	0.60	F	IF	N/A	N/A	-
B0143	BARS	0.58	H	I_1	Yes	No	-
B0144	BARS	0.51	Very Light green	SI_1	Yes	No	94 ± 15
B0145	BARS	0.46	F	SI_1	Yes	No	25 ± 4
B0146	BARS	0.40	E	SI_1	Yes	No	21 ± 3
B0147	BARS	0.40	F	SI_1	Yes	No	13 ± 2
B0148	BARS	0.31	Very Light yellowish green	VS_1	No	No	17 ± 3
B0149	BARS	0.30	G	VS_2	Yes	No	32 ± 5
B0150	BARS	0.30	Faint blue	VVS_1	Yes	No	26 ± 4
B0151	BARS	0.29	G	SI_2	Yes	No	13 ± 2
B0152	BARS	0.24	Faint yellow-green	VVS_1	No	Yes	4.3 ± 0.6
B0153	BARS	0.05	F	VVS_1	No	No	47 ± 7
B0154	BARS	0.05	H	VVS_1	No	No	-
B0155	BARS	0.05	E	VVS_1	No	No	30 ± 5
B0156	BARS	0.05	Faint blue	VVS_1	No	Yes	120 ± 20
B0157	BARS	0.05	D	VVS_2	No	No	49 ± 7
B0158	BARS	0.05	I	VVS_2	No	No	-
B0159	BARS	0.05	E	VVS_1	No	No	25 ± 4
B0160	BARS	0.05	E	IF	No	No	31 ± 5
B0161	BARS	0.05	F	VVS_1	No	No	100 ± 15
B0162	BARS	0.05	E	IF	No	No	23 ± 3
B4122	BARS	0.57	G	VS_1	No	No	4.1 ± 0.6
B4123	BARS	0.54	F	VVS_1	No	No	2.6 ± 0.4
B4124	BARS	0.50	Very Light blue	VS_2	Yes	Yes	90 ± 10
B4125	BARS	0.42	Faint blue	SI_1	Yes	Yes	42 ± 6
B4126	BARS	0.35	H	SI_1	Yes	No	-
B4127	BARS	0.33	Faint blue	SI_1	Yes	Yes	36 ± 5

[a] *$[B^0]$, averaged across the whole sample, was calculated using the integrated intensity of the 2800 cm^{-1} feature in the FTIR absorption data.*
N/A: not analyzed.

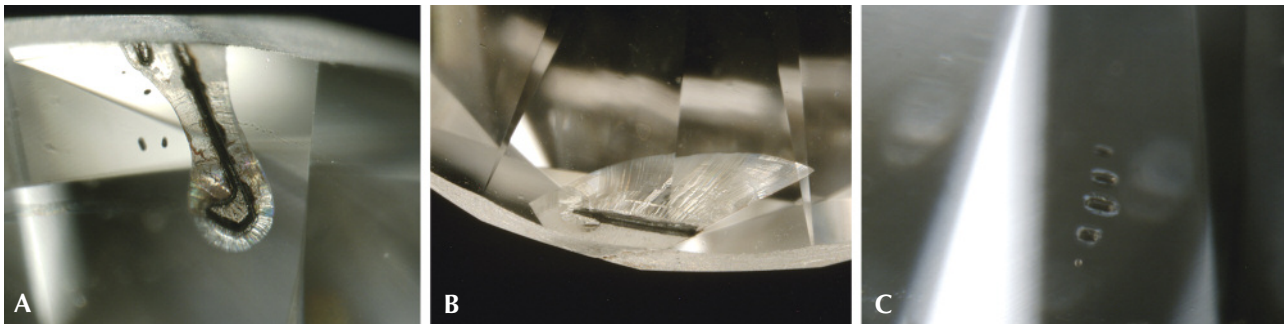

Figure 2. Some of AOTC's HPHT synthetic diamonds contained dark metallic inclusions, which were often rod-shaped. Surface-reaching feathers or fractures surrounding the inclusions were also observed. The photomicrographs for samples B0124 (A), B0143 (B), and B0149 (C) have image widths of 1.20, 2.40, and 1.05 mm, respectively. Inclusions in toroid-grown samples (not shown) were similar. Photomicrographs by Ulrika F.S. D'Haenens-Johansson.

ples received I_1–I_2 clarity grades. Graining was not observed in any of the AOTC samples. This is consistent with the subdued interference colors (gray/blue) displayed under crossed polarizers, as shown in figure 3, which indicate the low levels of strain characteristic of HPHT synthetic diamonds (Crowningshield, 1971). Higher levels of strain were only seen directly adjacent to inclusions or feathers.

Fluorescence and Phosphorescence. None of the samples showed fluorescence reactions under a handheld gemological long-wave UV lamp. Under short-wave UV, however, most displayed weak to strong greenish yellow fluorescence, with only 17% remaining inert. Fluorescence color zoning was not observed. The intensity of the fluorescence increased with exposure time, stabilizing after a few seconds. The fluorescing samples exhibited phosphorescence that was initially yellowish green but rapidly turned greenish blue. The greenish blue component was unusually long lasting, continuing for more than six minutes for some of the most intensely fluorescent samples. Stronger fluorescence to short-wave rather than long-wave illumination with a gemological lamp is one of the distinctive features of HPHT synthetic diamonds, as noted in the literature (Crowningshield, 1971; Koivula and Fryer, 1984; Rooney et al., 1993; Shigley et al., 1993, 1997). Fluorescence and phosphorescence colors were consistent with some of the near-colorless HPHT synthetic samples studied by Shigley et al. (1997).

DiamondView fluorescence images revealed cuboctahedral growth patterns typical of HPHT synthetics. The patterns form due to growth sector–dependent differences in a sample's impurity uptake, where a growth sector is defined as a three-dimensional region of the crystal with a common crystallographic growth plane (Burns et al., 1990, 1999). At

Figure 3. (A) Viewed between crossed polarizers, the AOTC samples displayed weak low-order interference colors and no discernible anomalous double refraction pattern, signifying very low levels of strain. Highly strained regions were only observed adjacent to fractures or inclusions, such as those shown in images B and C. These images are from samples B4123, B4127, and B0144, with image widths of 2.20, 2.65, and 1.25 mm, respectively. Photomicrographs by Ulrika F.S. D'Haenens-Johansson.

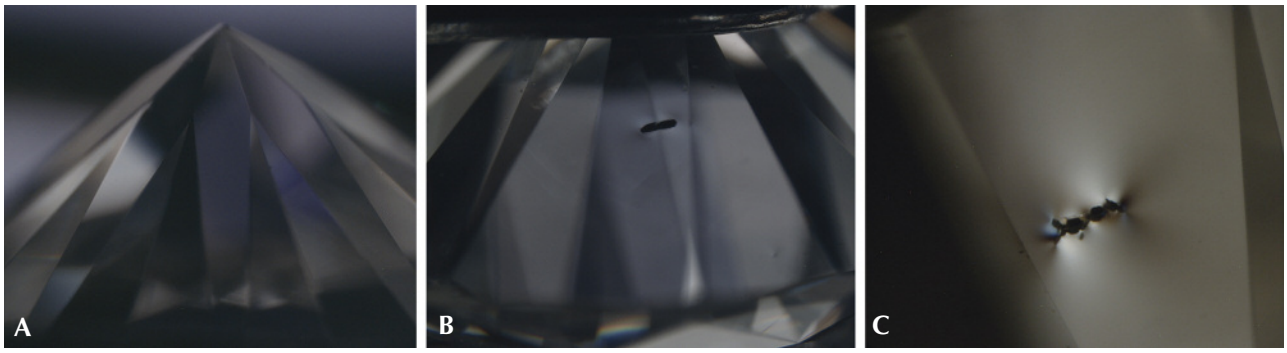

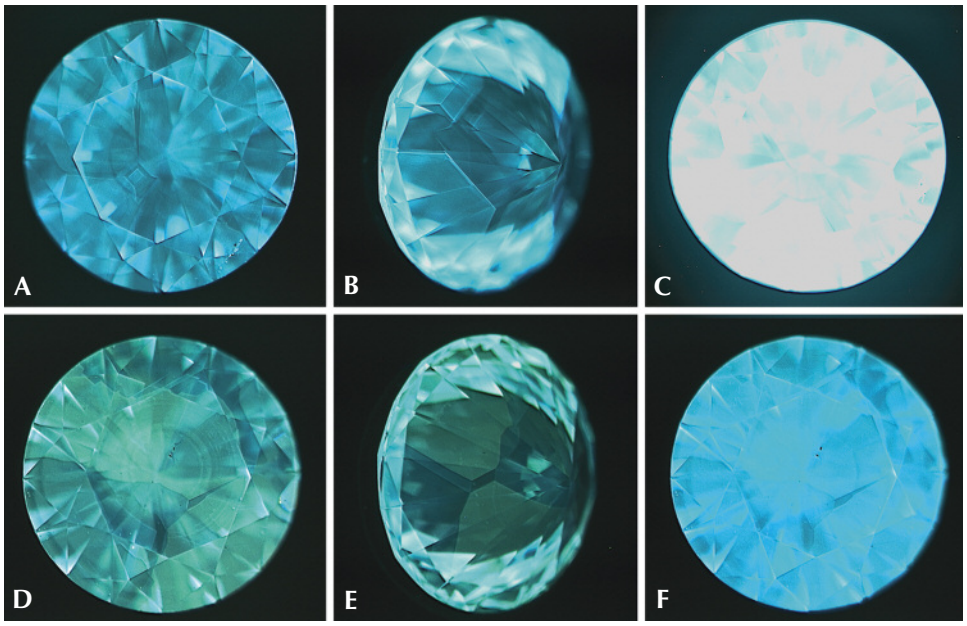

Figure 4. DiamondView images of samples B0124 (A–C) and B0148 (D–F). The fluorescence images (A, B, D, and E) show clear cuboctahedral patterns originating from their HPHT growth histories. The samples also displayed intense, long-lasting blue phosphorescence (C and F). These characteristics were observed for every AOTC sample. Images by Ulrika F.S. D'Haenens-Johansson.

times the contrast between adjacent fluorescing sectors was weak, and viewing such samples along multiple directions greatly aided in distinguishing the patterns. The bulk fluorescence was either blue or green, and the samples had strong blue phosphorescence, as illustrated in figure 4.

The phosphorescence behavior of the non-melee synthetic diamonds was further investigated using the previously described custom-built phosphorescence spectrometer. With each of these samples, the broadband illumination of the spectrometer (215–2500 nm) induced a blue phosphorescent emission centered at approximately 500 nm, as shown in figure 5. No other phosphorescence peaks were detected. The emission band at 500 nm (2.48 eV) has been reported in type IIb HPHT synthetic diamonds, but it can also be seen in natural type IIb diamonds (Watanabe et al., 1997; Eaton-Magaña et al., 2008; Eaton-Magaña and Lu, 2011). The phosphorescence is thought to arise from donor-acceptor pair recombination between the boron acceptor and unknown donors, possibly nitrogen defects (Dean, 1965, 1973; Klein et al., 1995; Watanabe et al., 1997). Note that even the nominally type IIa samples (see the Infrared Absorption Spectroscopy section below) displayed phosphorescence, suggesting the presence of boron impurities in concentrations below the FTIR spectrometer's detection limit.

Magnetism. All of the samples with SI_1–I_2 clarity grades were attracted to the rare-earth magnet, and most of the VS_2 samples were found to be weakly magnetic (see table 1). Past studies of gem-quality HPHT synthetics have demonstrated the magnetism of their inclusions (Koivula and Fryer, 1984; Rossman and Kirschvink, 1984). Most of the inclusions originate from the solvent/catalyst, which is typically a ferromagnetic material such as Fe or its alloys. Thus, depending on the inclusion size and number, and the proximity and strength of the magnet, HPHT synthetic diamonds may show magnetic

Figure 5. The room-temperature phosphorescence spectra for the non-melee synthetic diamonds showed strong emission at approximately 500 nm. The spectra have been vertically translated for clarity.

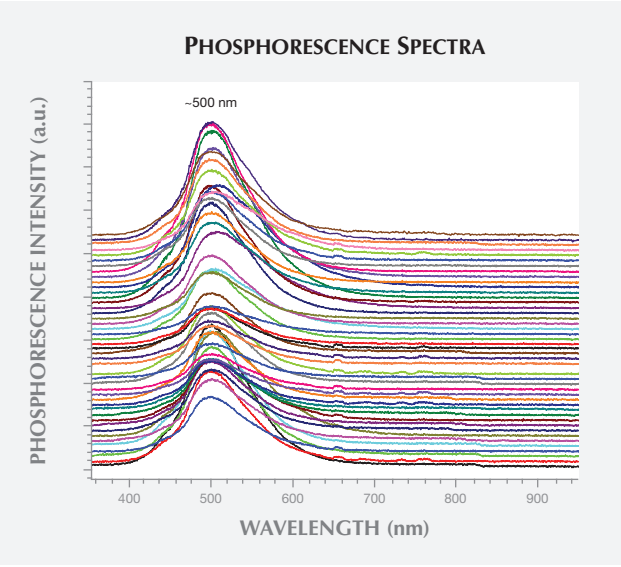

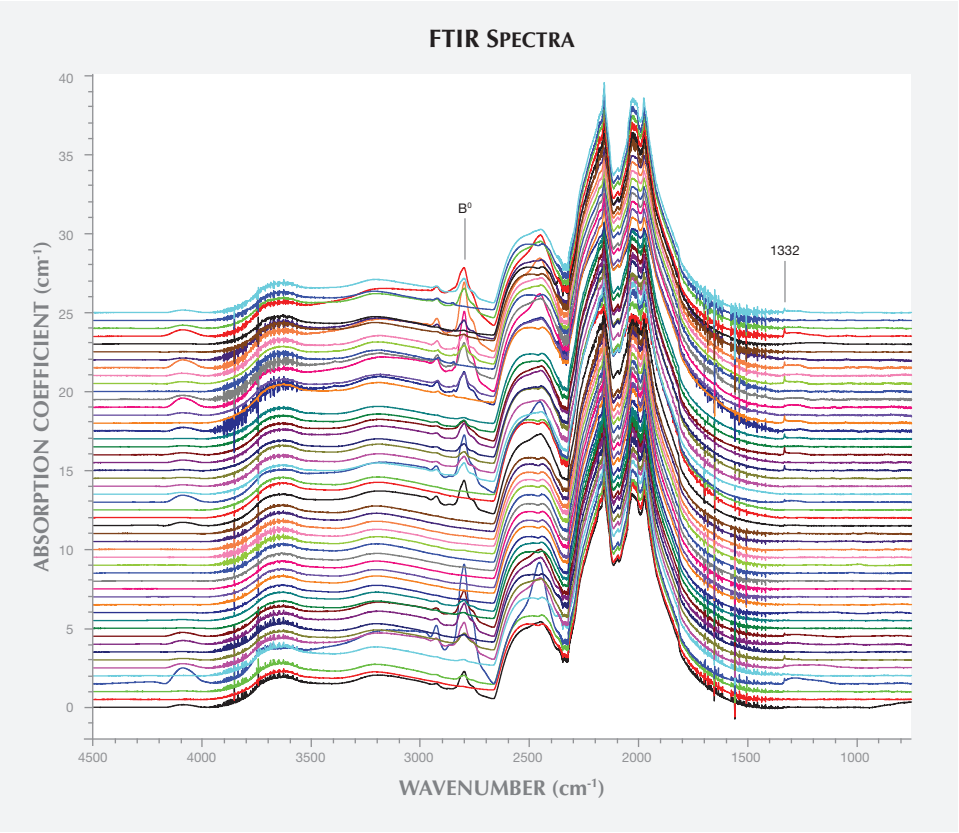

Figure 6. The FTIR spectra collected, translated vertically for clarity, revealed uncompensated boron absorption (B^0 at ~2800 cm^{-1}) and a weak peak at 1332 cm^{-1}. As a result, the AOTC samples were classified as mixed type IIa/IIb. The calculated bulk concentrations of B^0 are summarized in table 1.

attraction. It is extremely rare for the inclusions in a natural diamond to be attracted to a magnet (Koivula and Fryer, 1984), and CVD synthetics are not magnetic. Nevertheless, some diamonds, irrespective of their origin, demonstrate extremely weak magnetism due to surface contamination stemming from the cutting and polishing process. Careful cleaning will remove this effect (Rossman and Kirschvink, 1984). Magnetism is sometimes used to identify HPHT synthetic diamonds. If the synthetic diamonds do not contain significant inclusions, as was the case for 58% of the samples tested here, they will not be attracted to strong handheld magnets. Ultrasensitive equipment such as a superconducting quantum interference device (SQUID) may detect the magnetism of trace amounts of solvent/catalyst, but this is impractical for routine gemological investigations (Rossman and Kirschvink, 1984).

Electrical Conductivity. Electrical conductivity, occurring with white luminescence, was detected in some of the colored or lower-grade near-colorless samples, representing 17% of all the specimens tested (table 1). The conductivity measurements were found to depend on the positioning of the electrical probes on the samples. Some of the samples reported as not conductive, therefore, may have actually had conducting regions that were not accessed due to geometry or volume conditions. Electrical conductivity can indicate the presence of boron in diamond. The presence of boron turns pure insulating diamond into a conductive material. The solubility of boron is growth-sector dependent, and previous studies of boron-containing diamonds have shown that concentrations can vary in orders of magnitude across different growth sectors of the same specimen, with the highest concentrations usually found in {111} sectors. Yet the sector with the highest boron concentration has also been reported to be strongly influenced by the degree of doping (Burns et al., 1990). Hence, it is not surprising that boron-containing HPHT synthetic diamonds have sector-dependent electrical conductivity (Rooney et al., 1993; Shigley et al., 1997).

Infrared Absorption Spectroscopy. Infrared absorption spectroscopy revealed that the AOTC synthetic diamonds were mixed type IIa/IIb, or pure type IIa (figure 6). All the toroid samples belonged to the lat-

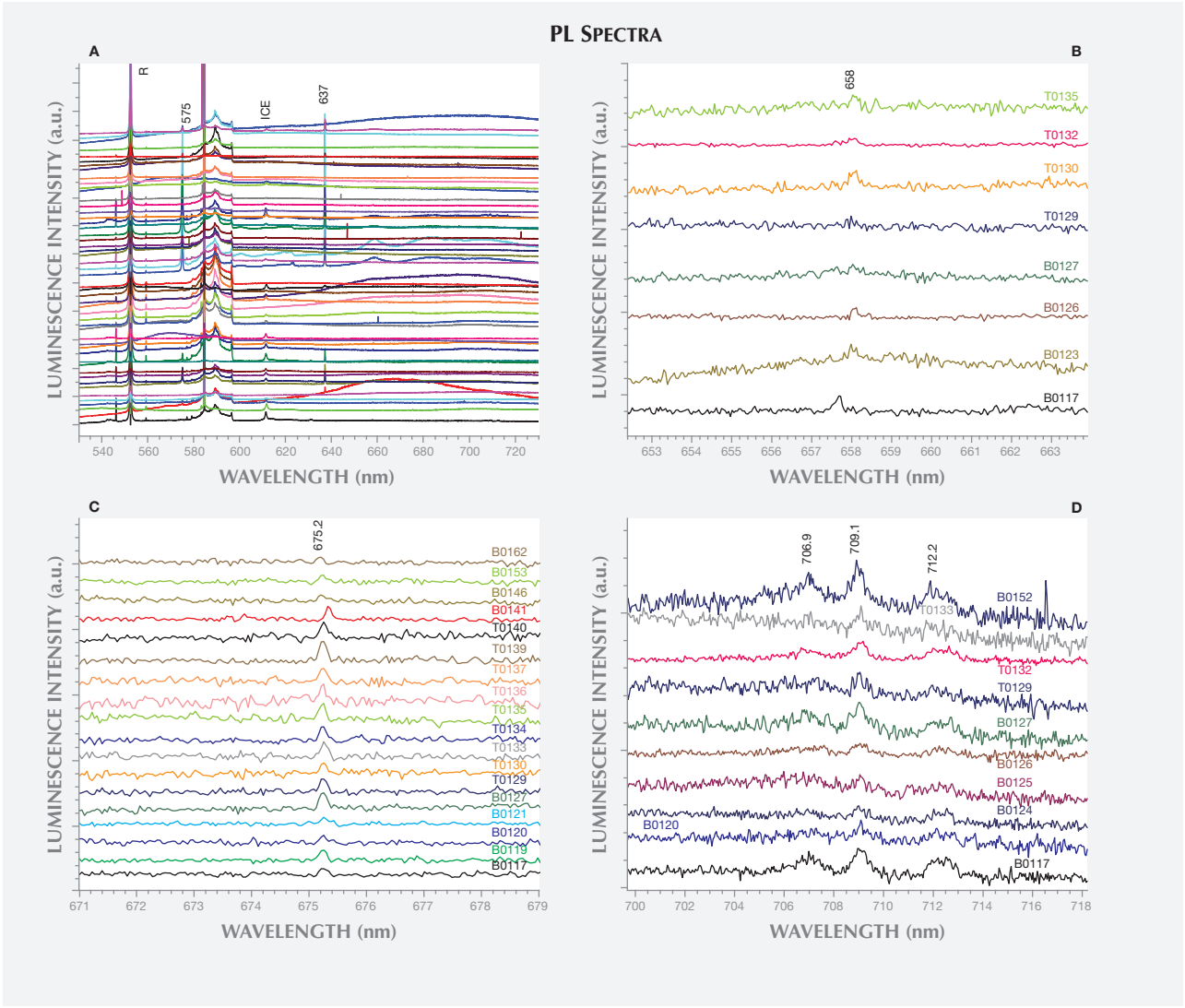

Figure 7. (A) PL spectra collected using 514.5 nm excitation were dominated by emission peaks from the NV^0 (575 nm) and NV^- (637 nm) centers. "R" denotes the diamond Raman peak. In certain samples, the 514.5 nm laser also excited weak peaks at 658.0 nm (B), 675.2 nm (C), and a group of peaks at 706.9, 709.1, and 712.2 nm (D). Representative spectra are shown and have been translated vertically for clarity.

ter classification, producing FTIR spectra that lacked any clear impurity-related absorption. The spectra for 34 of the 40 BARS samples revealed the presence of uncompensated boron (approximately 2800 cm^{-1}). The faceting of the samples made it impossible to isolate specific growth sectors for individual FTIR absorption measurements. Although boron is not uniformly distributed throughout these multi-sector HPHT synthetic diamonds, bulk concentrations – $[B^0]$ averaged across the whole sample volume – were calculated using the integrated intensities of the 2800 cm^{-1} feature, as described by Collins and Williams (1971) and Fisher et al. (2009). Regional boron concentrations will either be higher or lower than the bulk values, tabulated in table 1, but the estimates allow for semi-quantitative comparison between samples.

A weak peak at 1332 cm^{-1} was observed in 37 of the 40 BARS samples. Due to the high density of phonon states in this region, the identity of the 1332 cm^{-1} peak is uncertain, though it has been observed in boron-doped diamonds and in synthetic diamond grown using nickel-containing solvent/catalyst (Collins et al., 1990a; Lawson and Kanda, 1993; Lawson et al., 1998). The FTIR spectrum for the positively charged state of the substitutional nitrogen center (N_S^+) is characterized by a peak at 1332 cm^{-1} and broad features at 1046 and 950 cm^{-1} (Lawson et

al., 1998). As the latter two features were not observed in the AOTC samples' spectra, the 1332 cm^{-1} peak could not be attributed to this defect. Nor was the neutral charge state of substitutional nitrogen, N_S^0, which produces a peak at 1344 cm^{-1}, detected in any of the spectra (Lawson et al., 1998).

Photoluminescence. PL spectroscopy at liquid-nitrogen temperatures revealed no single peak in all of the samples, even though several contained similar defects (identified by their characteristic emission peaks). Since it was possible to excite emission from certain defects using multiple lasers, they will be described here for the lasers that caused the most efficient excitation (figures 7–10). In general, the observed emission peaks were weak, and could only be detected when the power was high enough to saturate the diamond Raman peak.

Nitrogen-vacancy center ($NV^{0/-}$) concentrations were sufficiently high in 33 of the 52 total samples to produce detectable zero-phonon lines (ZPLs) at 575 nm (2.156 eV, neutral charge state) or 637 nm (1.945 eV, negative charge state) with 514.5, 532.0, or 488.0 nm laser excitations. In the 514.5 nm PL spectra, the 637 nm ZPL was more intense than the 575 nm ZPL for 64% of the samples showing these emissions (see figures 7A–D). These spectra also revealed weak unidentified peaks at 658.0 nm (1.884 eV) in 19 of the samples and at 675.2 nm (1.836 eV) in 9 samples (37% and 17%, respectively). Additionally, a set of faint emission lines at 706.9, 709.1, and 712.2 nm (1.754, 1.748, and 1.741 eV) was observed in 12 of the samples (23%). It is unknown whether these are related.

Overall, the synthetic diamonds grown by AOTC using toroid-press systems showed remarkably few (and weak) PL features, limited to those discussed above. The remaining laser excitation wavelengths did not induce any other defect-related emissions. Sample T0131 was exceptionally pure and did not have any detectable optical centers. Conversely, several of the diamonds synthesized using BARS-press technology showed additional ZPLs. Any other peaks discussed hereafter were only detected in this group of 40 BARS samples.

A weak peak at 503.2 nm (2.463 eV), possibly H3 ($N\text{-}V\text{-}N^0$), was detected in the 488.0 nm laser-excited PL spectra for 11 of the BARS samples (27.5%). Emission at this wavelength has previously been reported in both type IIa and IIb HPHT-grown synthetic diamonds (Dodge, 1986; Collins et al., 1990a; Sittas et al., 1996; Zaitsev, 2001).

As shown in figure 8, the negatively charged silicon split-vacancy defect, with a doublet ZPL at 736.6/736.9 nm (SiV^-, 1.683 eV), was clearly resolved in the 632.8 nm PL spectra for four samples (10%). This is surprising, as the presence of silicon (Si) is rarely reported in HPHT synthetic diamond. Intentional Si-doping occurred in the studies by Clark et al. (1995) and Sittas et al. (1996), where Si was added to the Fe, Fe-Ni, or Fe-Co solvent/catalyst mixture; the latter study also included Ti or Zr nitrogen getters. Si-doping by post-growth Si^+ implantation has also been reported (Collins et al., 1990b). To date, SiV^- has only been reported twice for faceted gem-quality HPHT synthetics, but it is unknown whether its presence was intentional or simply a byproduct of contamination (Moe and Wang, 2010; Wang and Moe, 2012).

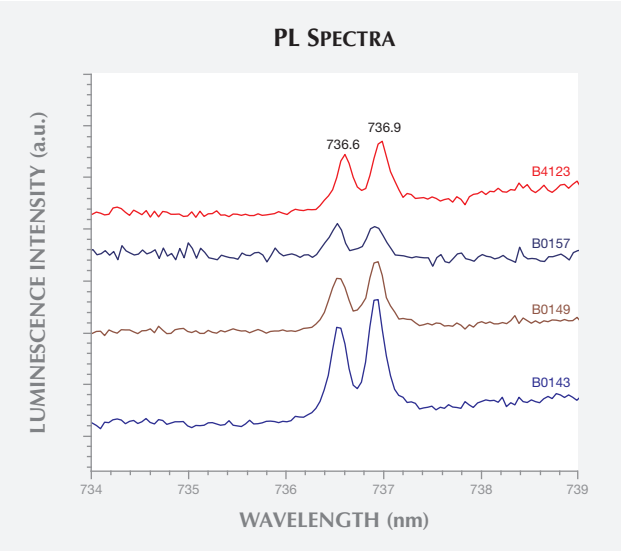

Figure 8. The SiV^- center, with emission peaks at 736.6 and 736.9 nm, was observed in the PL spectra for four samples using 632.8 nm laser excitation. Spectra have been translated vertically for clarity.

A doublet at 882.6/884.3 nm (1.405/1.402 eV), excited using the 830.0 nm laser, was the most commonly observed ZPL, detected in 28 (70%) of the BARS samples (figure 9). This doublet, typically referred to as the 1.40 eV center, is frequently seen using absorption or PL spectroscopy in the {111} growth sectors of HPHT synthetic diamonds produced using Ni-based solvent/catalysts (Collins et al., 1990a; Nazaré et al., 1991; Collins, 1992; Lawson and Kanda, 1993). Nazaré et al. were able to resolve the fine structure for the band and conducted uniaxial stress and Zeeman splitting measurements, conclusively determining that the defect responsible contains a single Ni atom (Davies et al., 1989). The splitting between the dominant 882.6 and 884.3 nm lines was found to rise with increasing linewidths,

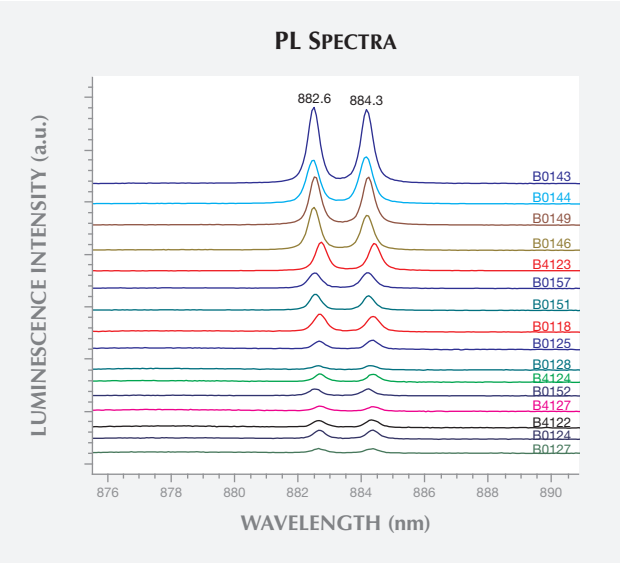

Figure 9. A Ni-related doublet at 882.6 and 884.3 nm was detected in most of the PL spectra (830.0 nm laser excitation) collected for the BARS samples. These representative spectra have been translated vertically for clarity.

which follow increasing strain levels. They hypothesized that the ZPL originates at an interstitial Ni^+ atom distorted along a ⟨111⟩ direction. Although this is the most widely accepted model, it has not been unambiguously confirmed (Yelisseyev and Kanda, 2007).

Figure 10. The 484 nm center, with peaks at 483.59, 483.84, 484.11, and 484.45 nm, was detected in the PL spectra (324.8 nm laser excitation) of 10 of the 40 BARS-grown samples. Only the most intense and clearly resolved spectra are presented here, translated vertically for clarity.

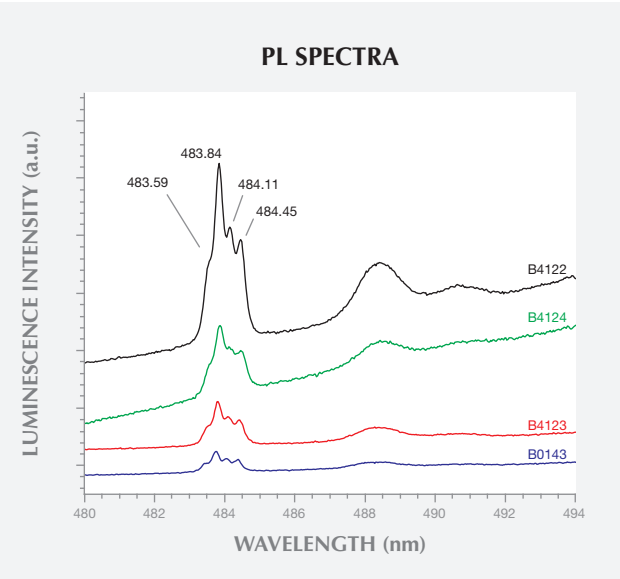

The 324.8 nm laser excitation PL spectra in figure 10 revealed the presence of a complex luminescence system, centered at about 484 nm in 10 of the 40 BARS samples. This band, referred to as the 484 nm or 2.56 eV center, is frequently observed in the absorption or PL (excitation wavelength <400 nm) spectra of Ni-doped HPHT synthetic diamonds. Like the 882.6/884.3 nm doublet, it is mainly restricted to {111} growth sectors (Dean, 1965; Collins et al., 1990a; Collins, 1992). The band consists of peaks at 483.59, 483.84, 484.11, and 484.45 nm (2.564, 2.563, 2.561, and 2.559 eV) resulting from the splitting of the excited state. The 883.6/884.3 nm optical center was detected in the PL spectra for every AOTC sample that also contained the 484 nm center. The PL spectra acquired using the 457.0 and 532.0 nm laser excitations did not reveal any additional photoluminescent centers.

LA-ICP-MS. The LA-ICP-MS data collected on the surface-reaching inclusions of samples B0124 and T0130, thought to be remnants of the solvents/catalysts used during growth, provided clues to their growth capsule constituents. B0124 and T0130 were synthesized using BARS- and toroid-press technologies, respectively. The raw data are presented in figure 11, where the number of counts detected for certain elements were monitored as a function of time: before, during, and after the inclusion was vaporized by the laser. It is important to note that the sensitivity of LA-ICP-MS to different elements is not uniform, so these plots should not be compared for distinct elements. Conventionally, quantitative concentration analysis can be achieved by comparing the intensity of the detected counts for each element with that for a reference sample with known, calibrated element concentrations. The large variance (at times multiple orders of magnitude) in the concentration of different elements between the inclusions and the reference samples introduced uncertainties significant enough that quantitative analysis of relative concentrations was not deemed suitable. Nevertheless, the LA-ICP-MS data proved reliable in determining the presence of certain elements in the inclusion.

The metallic inclusions in samples B0124 and T0130 clearly contained Fe and Zr, and a weak signal was detected from Cu. Sample B0124's inclusion also contained Hf and Co, while T0130 showed considerable levels of Al. Ni, whose presence was identified by the PL data for B0124, was not detected in either

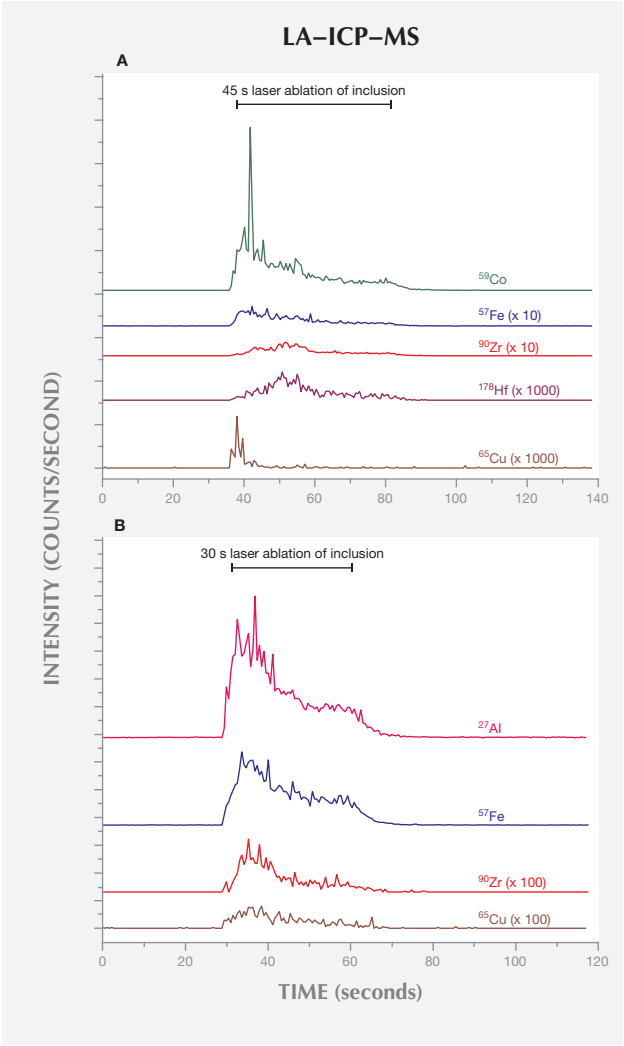

Figure 11. LA-ICP-MS data for the inclusions in samples B0124 (A) and T0130 (B), which were grown using BARS- and toroid-press technologies, respectively. The traces have been scaled and vertically translated for clarity.

sample. This is likely a result of relatively poor detection limits for Ni with LA-ICP-MS instruments such as the X-Series II, which use skimmer cones made of Ni. Fe and Co are commonly used in the solvent/catalyst mixtures for HPHT synthetic diamond growth. Al, Zr, and Hf have been previously used as nitrogen getters for HPHT diamond synthesis, while Cu can be used to reduce the formation of carbides such as ZrC (Strong and Chrenko, 1971; Burns et al., 1990; Sumiya and Satoh, 1996; Sumiya et al., 1996).

DISCUSSION

Improvements by AOTC in Gem-Quality HPHT Synthetic Diamonds. The growth of colorless HPHT synthetic diamonds for faceting on a commercial scale has proven extremely complex. The primary challenges have been to exclude readily incorporated nitrogen impurities, while simultaneously achieving acceptable growth rates and minimizing the incorporation of the solvent/catalyst melt, which forms unattractive inclusions. Sophisticated presses with accurate long-term temperature and pressure controls are necessary, in conjunction with a carefully selected combination of carbon source, nitrogen getter, and solvent/catalyst. Previous efforts to manufacture similarly colored material by this method have been limited by technological or economic constraints; successful fabrication has been done primarily for research purposes or niche industrial applications (Crowningshield, 1971; Rooney et al., 1993; Shigley et al., 1993, 1997; Sumiya and Satoh, 1996; Sumiya et al., 2002).

The overall quality of the AOTC samples was remarkably high, with 77% of the suite assigned colorless to near-colorless grades. Furthermore, the specimens reached sizes that are popular with the jewelry consumer, with the largest sample weighing 0.80 ct. Clarity, which ranged from IF to I_2, was typically affected by the presence of dark inclusions originating from the solvent/catalyst melt. The clarity grades did not strictly correlate with size or color, though the melee-size specimens were generally of higher clarity. Overall, the clarities seen in these colorless and near-colorless HPHT synthetics are considerably better than most previous products. This combination of color, size, and clarity makes the AOTC products, on first inspection, comparable to natural and CVD synthetic diamonds on the market.

Characterization using PL, FTIR absorption, and LA-ICP-MS has provided a body of data that allows us to speculate about the identity of some key chemical components present during the HPHT synthesis of the samples and comment on the resulting gemological characteristics. FTIR data demonstrated that most of the BARS-press synthetics contained extremely low levels of boron impurities and no detectable levels of isolated nitrogen defects. The low concentration of nitrogen defects indicates the use of a nitrogen getter during growth. The yellow color often associated with HPHT synthetic diamonds arises from typically high concentrations of neutrally charged substitutional nitrogen. Neutral substitutional nitrogen was not detected in the AOTC samples, which explains the absence of a yellow hue. On the other hand, the neutral boron that was detected can introduce a blue hue. The color ultimately

achieved is affected by not only the concentration of the different color-producing defects, but also by the diamond's volume and faceting arrangement. Overall, synthetic diamonds with low boron concentrations were likely to appear colorless to near-colorless, while the samples with higher boron concentrations tended to show enough saturation of blue color to be graded using the fancy color scale. In all likelihood, a combination of color-producing defects was responsible for the non-blue colors observed in a small subset of the samples.

PL spectroscopy revealed that 70% of the samples grown using BARS presses contained Ni-related impurities. Ni is frequently used in the solvent/catalyst mixture, as it reduces the temperature and pressure conditions needed for diamond synthesis. Conversely, there was no evidence for the incorporation of Ni in any of the samples produced by toroid presses. This suggests the use of a different solvent/catalyst mixture for the two press types. Unfortunately, PL-active defects produced by Fe or Co, elements that are often constituents of the solvent/catalyst, have not yet been identified in as-grown HPHT synthetic diamond. While a few Co-related PL features have been reported in annealed synthetic diamonds, they were limited to samples with significant nitrogen contamination (Lawson et al., 1996). The AOTC samples had nitrogen concentrations below the FTIR spectrometer's detection limit and reportedly have not undergone post-growth treatment (D.NEA, 2014b). Hence, PL cannot be used to confirm or rule out the presence of Fe or Co. It is unknown whether the presence of SiV^- in the PL spectra for four of the BARS-press samples arose from intentional Si-doping, but the low concentration suggests that it resulted from contamination.

Notably, the samples produced by toroid presses showed uncommonly faint and limited features in their PL spectra. This result, combined with the absence of detectable defect-related absorption in their FTIR spectra, suggests that AOTC has exerted more control over impurity incorporation in its toroid-press production. These samples, however, were more likely to contain significant inclusions from the solvent/catalyst melt.

LA-ICP-MS analysis of inclusions in samples grown using the two different press types revealed additional information. Although only two samples were analyzed, and caution must be taken when extrapolating the results to AOTC's entire commercial production, the gemological and spectroscopic properties were consistent with the remaining samples from the two press types. The inclusions' chemical composition provides strong indications about the solvent catalysts and nitrogen getters used during synthesis in the two different presses. Our chemical data suggest that the BARS press employed some combination of Fe, Co, and Ni in the solvent catalyst; Zr and Hf as nitrogen getters; and Cu to reduce inclusions. For the toroid press, we saw evidence of the addition of Zr and Al as nitrogen getters and Cu to reduce inclusions, but it remains unclear what other elements besides Fe constituted the solvent catalyst. If present, Co and Ni were likely much lower in concentration in the toroid growth process. Additional analysis is necessary to constrain this further.

Identification Features. Similar to previous reports on HPHT synthetic diamond from other manufacturers, certain visual characteristics can be used to characterize the AOTC samples as HPHT synthetic, although advanced testing is necessary for conclusive identification. Due to the high color grades of the AOTC product, visual inspection did not reveal patterned color zoning arising from their cuboctahedral growth morphology. Under magnification, unusual elongated, dark metallic solvent/catalyst inclusions, similar to those often seen in other HPHT synthetic diamonds, were observed in some samples. If heavily included, the AOTC synthetics were also attracted to a strong magnet, confirming the presence of ferrous material not associated with natural diamonds. The shape and metallic appearance of the inclusions are an extremely rare combination in natural diamonds, and should therefore arouse suspicion (Sobolev et al., 1981). When viewed between crossed polarizers, AOTC's HPHT synthetics also showed remarkably low levels of strain without a discernible pattern. This is in contrast to natural diamonds, which typically show cross-hatched "tatami," banded, or mottled strain patterns.

Illumination with a standard gemological UV lamp produced a yellowish green fluorescence and phosphorescence to short-wave UV, while the samples were inert to long-wave UV. The stronger response to short-wave UV is the opposite of the reaction observed for most natural diamonds (Shigley et al., 1993). The intense, long-lasting phosphorescence induced in some of the AOTC synthetics is seldom observed in natural diamonds and should alert the gemologist to the need for more detailed analysis. Fancy-color HPHT synthetic diamonds often display a fluorescence zoning arising from the variation in the uptake of impurities for the different growth sectors. In this study, the contrast

was too low to be detected using a handheld UV lamp. Only the high-energy UV excitation and magnification-enabled imaging of the DiamondView instrument revealed the cuboctahedral growth patterns characteristic of HPHT synthetics.

FTIR spectra characterized the AOTC synthetic diamonds as type IIa/IIb, without any features exclusive to HPHT synthetics. Since the majority of natural near-colorless diamonds are type IaA, however, all type IIa or IIb samples should be treated with caution and subjected to additional testing. PL spectroscopy was able to demonstrate the presence of Ni-related impurities in most of the BARS-press samples, which displayed distinctive lines at 882.6/884.3 nm and a band of four lines centered at about 484.0 nm. It is important to note that Ni-related defects are rarely detected in natural diamonds (Nobel et al., 1998; Chalain, 2003; unpublished GIA research), and their presence should immediately raise suspicion. Significantly, these features were absent in the PL spectra of AOTC's toroid-press synthetic diamonds.

Other useful peaks at 658.0, 675.2, 706.9, 709.1, and 712.2 nm were seen in some samples, from both BARS- and toroid-type presses. These peaks have not previously been reported and are thus promising for identification purposes. The detection of the SiV^- optical center at 736.6/736.9 nm in four AOTC samples, in addition to a number of natural and HPHT-grown synthetic diamonds (Breeding and Wang, 2008; Moe and Wang, 2010; Wang and Moe, 2012), emphasizes that this feature should not be considered proof of CVD synthesis. Overall, the high purity levels of the AOTC synthetics resulted in PL features that were usually much weaker than the diamond Raman peak, requiring a high-sensitivity spectrometer for detection.

CONCLUSION

The high quality and excellent colors achieved by AOTC's latest HPHT synthetic diamonds represent an important milestone, as well as a new challenge for identification. No longer can a gemologist assume that colorless HPHT synthetics will contain abundant metallic inclusions. Analysis of a suite of 52 specimens from this manufacturer has underscored the fact that conclusive identification of synthetics cannot be made simply using a single gemological or spectroscopic method. Fortunately, the tools available to the average gemologist will enable recognition of features that may imply a synthetic origin, and alert them to the need for additional advanced testing by a gemological laboratory. By combining a variety of gemological, spectroscopic, and fluorescence imaging techniques, all of the AOTC samples could be unequivocally recognized as HPHT synthetic diamonds.

ABOUT THE AUTHORS

Dr. D'Haenens-Johansson (ujohansson@gia.edu) is a research scientist, Mr. Moe is a research associate, Mr. Johnson is the supervisor of diamond advanced testing, and Dr. Wang is the director of research and development at GIA's New York laboratory. Ms. Wong is a diamond grader in GIA's Hong Kong laboratory. Prof. Lu, formerly a senior research scientist at GIA, is a professor at the Wuhan Geological University in China.

ACKNOWLEDGMENTS

The authors would like to thank Mr. Erik Franklin, CEO of D.NEA, for providing us with the samples used in this study.

REFERENCES

Bovenkerk H.P., Bundy F.P., Hall H.T., Strong H.M., Wentorf R.H. (1959) Preparation of diamond. *Nature*, Vol. 184, No. 4693, pp. 1094–1098, http://dx.doi.org/10.1038/1841094a0.

Breeding C.M., Wang W. (2008) Occurrence of the Si-V defect center in natural colorless gem diamonds. *Diamond and Related Materials*, Vol. 17, Nos. 7–10, pp. 1335–1344, http://dx.doi.org/10.1016/j.diamond.2008.01.075.

Bundy F.P., Hall H.T., Strong H.M., Wentorf R.H. (1955) Man-made diamonds. *Nature*, Vol. 176, No. 4471, pp. 51–55, http://dx.doi.org/10.1038/176051a0.

Bundy F.P., Strong H.M., Wentorf R.H. Jr. (1973) Methods and mechanisms of synthetic diamond growth. *Chemistry and Physics of Carbon*, Vol. 10, pp. 213–263.

Burns R.C., Cvetkovic V., Dodge C. N., Evans D.J.F., Rooney M.-L.T., Spear P.M., Welbourn C.M. (1990) Growth-sector dependence of optical features in large synthetic diamonds. *Journal of Crystal Growth*, Vol. 104, No. 2, pp. 257–279, http://dx.doi.org/10.1016/0022-0248(90)90126-6.

Burns R.C., Hansen J.O., Spits R.A., Sibanda M., Welbourn C.M., Welch D.L. (1999) Growth of high purity large synthetic diamond crystals. *Diamond and Related Materials*, Vol. 8, Nos. 8–9, pp. 1433–1437, http://dx.doi.org/10.1016/S0925-9635(99)00042-4.

Chalain J.P. (2003) Gem News International: A natural yellow diamond with nickel-related optical centers. *G&G*, Vol. 39, No. 4, pp. 325–326.

Chrenko R.M., Strong H.M., Tuft R.E. (1971) Dispersed paramagnetic nitrogen content of large laboratory diamonds. *Philosophical Magazine*, Vol. 23, No. 182, pp. 313–318, http://dx.doi.org/10.1080/14786437108216387.

Chrenko R.M., Tuft R.E., Strong H.M. (1977) Transformation of the state of nitrogen in diamond. *Nature*, Vol. 270, No. 5633, pp. 141–144, http://dx.doi.org/10.1038/270141a0.

Clark C.D., Kanda H., Kiflawi I., Sittas G. (1995) Silicon defects in diamond. *Physical Review B*, Vol. 51, No. 23, pp. 16681–16688, http://dx.doi.org/10.1103/PhysRevB.51.16681.

Collins A.T. (1992) The characterisation of point defects in diamond by luminescence spectroscopy. *Diamond and Related Materials*, Vol. 1, Nos. 5–6, pp. 457–469, http://dx.doi.org/10.1016/0925-9635(92)90146-F.

Collins A.T., Kanda H., Burns R.C. (1990a) The segregation of nickel-related optical centers in the octahedral growth sectors of synthetic diamond. *Philosophical Magazine Part B*, Vol. 61, pp. 797–810.

Collins A.T., Kamo M., Sato, Y. (1990b) A spectroscopic study of optical centers in diamond grown by microwave-assisted chemical vapor deposition. *Journal of Materials Research*, Vol. 5, No. 11, pp. 2507–2514, http://dx.doi.org/10.1557/JMR.1990.2507.

Collins A.T., Williams A.W.S. (1971) The nature of the acceptor centre in semiconducting diamond. *Journal of Physics C: Solid State Physics*, Vol. 4, No. 13, pp. 1789–1800, http://dx.doi.org/10.1088/0022-3719/4/13/030.

Crowningshield R. (1971) General Electric's cuttable synthetic diamonds. *G&G*, Vol. 13, No. 10, pp. 302–314.

Davies G., Neves A.J., Nazaré M.H. (1989) Nickel isotope effects in the 1.4 eV center in synthetic diamond. *Europhysics Letters*, Vol. 9, No. 1, pp. 47–52.

Dean P.J. (1965) Bound excitons and donor-acceptor pairs in natural and synthetic diamond. *Physical Review*, Vol. 139, No. 2A, pp. A588–A602, http://dx.doi.org/10.1103/PhysRev.139.A588.

Dean P.J. (1973) Inter-impurity recombinations in semiconductors. *Progress in Solid State Chemistry*, Vol. 8, pp. 1–126, http://dx.doi.org/10.1016/0079-6786(73)90004-6.

Deljanin B., Simic D., Epelboym M., Zaitsev A.M. (2006) Study of fancy-color and near-colorless HPHT-grown synthetic diamonds from Advanced Optical Technology Co., Canada. *G&G*, Vol. 42, No. 3, pp. 154–155.

D'Haenens-Johansson U.F.S., Moe K.S., Johnson P., Wong S.Y., Wang W. (2012) Lab Notes: Near-colorless HPHT-grown synthetic diamonds from Advanced Optical Technology Co. *G&G*, Vol. 48, No. 2, p. 141.

D.NEA (2014a) Identify a created diamond. http://d.neadiamonds.com/identify-a-created-diamond [date accessed: Feb. 18, 2014].

D.NEA (2014b) Synthetic white diamonds (colorless). http://d.neadiamonds.com/white-diamond [date accessed: Feb. 18, 2014].

D.NEA (2014c) Diamond prices. http://d.neadiamonds.com/diamond-price [date accessed: Feb. 18, 2014].

D.NEA (2014d) Synthetic yellow diamond. http://d.neadiamonds.com/yellow-diamond [date accessed Mar. 25, 2014).

D.NEA (2014e) Synthetic blue diamond. http://d.neadiamonds.com/blue-diamond [date accessed Mar. 25, 2014).

Dodge C. (1986) An optical study of sintered and black diamond. Ph.D. thesis, University of Reading, UK.

Eaton-Magaña S., Lu R. (2011) Phosphorescence in type IIb diamonds. *Diamond and Related Materials*, Vol. 20, No. 7, pp. 983–989, http://dx.doi.org/10.1016/j.diamond.2011.05.007.

Eaton-Magaña S., Post J.E., Heaney P.J., Walters R.A., Breeding C.M., Butler J.E. (2007) Fluorescence spectra of colored diamonds using a rapid, mobile spectrometer. *G&G*, Vol. 43, No. 4, pp. 332–351, http://dx.doi.org/10.5741/GEMS.43.4.332.

Eaton-Magaña S., Post J., Heaney P.J., Freitas J., Klein P., Walters R., Butler J.E. (2008) Using phosphorescence as a fingerprint for the Hope and other blue diamonds. *Geology*, Vol. 36, No. 1, pp. 83–86, http://dx.doi.org/10.1130/G24170A.1.

Even-Zohar C. (2012) Synthetics specifically 'made to defraud.' *Diamond Intelligence Briefs*, Vol. 27, No. 709, pp. 7281–7283.

Fisher D., Sibley S.J., Kelly C.J. (2009) Brown colour in natural diamond and interaction between the brown related and other colour-inducing defects. *Journal of Physics: Condensed Matter*, Vol. 21, No. 36, 364213, 10 pp., http://dx.doi.org/10.1088/0953-8984/21/36/364213.

Khvostantsev L.G., Slesarev V.N., Brazhkin V.V. (2004) Toroid type high-pressure device: History and prospects. *High Pressure Research*, Vol. 24, No. 3, pp. 371–383, http://dx.doi.org/10.1080/08957950412331298761.

Klein P.B., Crossfield M.D., Freitas J.A., Collins A.T. (1995) Donor-acceptor pair recombination in synthetic type-IIb semiconducting diamond. *Physical Review B*, Vol. 51, No. 15, pp. 9634–9642, http://dx.doi.org/10.1103/PhysRevB.51.9634.

Koivula J.I., Fryer C.W. (1984) Identifying gem-quality synthetic diamonds: An update. *G&G*, Vol. 20, No. 3, pp. 146–158, http://dx.doi.org/10.5741/GEMS.20.3.146.

Koivula J.I., Kammerling R.C., Fritsch E., Eds. (1994) Gem News International: Near-colorless synthetic diamond examined. *G&G*, Vol. 30, No. 2, pp. 193–194.

Lawson S.C., Kanda H. (1993) An annealing study of nickel point defects in high-pressure synthetic diamond. *Journal of Applied Physics*, Vol. 73, No. 8, pp. 3967–3973, http://dx.doi.org/10.1063/1.352861.

Lawson S.C., Kanda H., Watanabe K., Kiflawi I., Sato Y., Collins A.T. (1996) Spectroscopic study of cobalt-related optical centers in synthetic diamond. *Journal of Applied Physics*, Vol. 79, No. 8, pp. 4348–4357, http://dx.doi.org/10.1063%2F1.361744.

Lawson S.C., Fisher D., Hunt D.C., Newton M.E. (1998) On the existence of positively charged single-substitutional nitrogen in diamond. *Journal of Physics: Condensed Matter*, Vol. 10, No. 27, pp. 6171–6180, http://dx.doi.org/10.1088/0953-8984/10/27/016.

Moe K.S., Wang W. (2010) Lab Notes: Silicon-vacancy defect found in blue HPHT-grown synthetic diamond. *G&G*, Vol. 46, No. 4, p. 302.

Nazaré M.H., Neves A.J., Davies G. (1991) Optical studies of the 1.40-ev Ni center in diamond. *Physical Review B*, Vol. 43, No. 17, pp. 14196–14205, http://dx.doi.org/10.1103/PhysRevB.43.14196.

Noble C.J., Pawlik T., Spaeth J.-M. (1998) Electron paramagnetic resonance investigations of nickel defects in natural diamonds. *Journal of Physics: Condensed Matter*, Vol. 10, No. 50, pp. 11781–11794, http://dx.doi.org/10.1088/0953-8984/10/50/017.

Palik E.D. (1985) *Handbook of Optical Constants of Solids*. Academic Press, London.

Rooney M.-L.T., Welbourn C.M., Shigley J.E., Fritsch E., Reinitz I. (1993) De Beers near colorless-to-blue experimental gem-quality synthetic diamonds. *G&G*, Vol. 29, No. 1, pp. 38–45, http://dx.doi.org/10.5741/GEMS.29.1.38.

Rossman G.R., Kirschvink J.I. (1984) Magnetic properties of gem-quality synthetic diamonds. *G&G*, Vol. 20, No. 3, pp. 163–166, http://dx.doi.org/10.5741/GEMS.20.3.163.

Shigley J.E., Fritsch E., Reinitz, I. (1993a) Two near-colorless General Electric Type-IIa synthetic diamond crystals. *G&G*, Vol. 29, No. 3, pp. 191–197, http://dx.doi.org/10.5741/GEMS.29.3.191.

Shigley J.E., Fritsch E., Koivula J.I., Sobolev N.V., Malinovsky I.Y., Pal'yanov Y.N. (1993b) The gemological properties of Russian gem-quality synthetic diamonds. *G&G*, Vol. 29, No. 4, pp. 228–248, http://dx.doi.org/10.5741/GEMS.29.4.228.

Shigley J.E., Moses T.M., Reinitz I., Elen S., McClure S.F., Fritsch E. (1997) Gemological properties of near-colorless synthetic diamonds. *G&G*, Vol. 33, No. 1, pp. 42–53, http://dx.doi.org/10.5741/GEMS.33.1.42.

Shigley J.E., Abbaschian R., Clarke C. (2002) Gemesis laboratory-created diamonds. *G&G*, Vol. 38, No. 4, pp. 301–309, http://dx.doi.org/10.5741/GEMS.38.4.301.

Sittas G., Kanda H., Kiflawi I., Spear P.M. (1996) Growth and characterization of Si-doped diamond single crystals grown by the HTHP method. *Diamond and Related Materials*, Vol. 5, Nos. 6–8, pp. 866–869, http://dx.doi.org/10.1016/0925-9635(95)00449-1.

Sobolev N.V., Efimiva E.S., Pospelova L.N. (1981) Native iron in diamonds of Yakutia and its paragenesis. *Soviet Geology and Geophysics*, Vol. 22, No. 12, pp. 18–21.

Strong H.M., Chrenko R.M. (1971) Further studies on diamond growth rates and physical properties of laboratory-made dia-

mond. *The Journal of Physical Chemistry*, Vol. 75, No. 12, pp. 1838–1843, http://dx.doi.org/10.1021/j100681a014.
Sumiya H., Satoh S. (1996) High-pressure synthesis of high-purity diamond crystal. *Diamond and Related Materials*, Vol. 5, pp. 1359–1365, http://dx.doi.org/10.1016/0925-9635(96)00559-6.
Sumiya H., Toda N., Satoh S. (2002) Growth rate of high-quality large diamond crystals. *Journal of Crystal Growth*, Vol. 237–239, Part 2, pp. 1281–1285, http://dx.doi.org/10.1016/S0022-0248(01)02145-5.
Sumiya H., Toda N., Satoh S. (2005) Development of high-quality large-size synthetic diamond crystals. *SEI Technical Review*, Vol. 60, pp. 10–16.
Wang W., Hall M.S., Moe K.S., Tower J., Moses T.M. (2007) Latest-generation CVD-grown synthetic diamonds from Apollo Diamond Inc. *G&G*, Vol. 43, No. 4, pp. 294–312, http://dx.doi.org/10.5741/GEMS.43.4.294.
Wang W., D'Haenens-Johansson U.F.S., Johnson P., Moe K.S., Emerson E., Newton M.E., Moses T.M. (2012) CVD synthetic diamonds from Gemesis Corp. *G&G*, Vol. 48, No. 2, pp. 80–97, http://dx.doi.org/10.5741/GEMS.48.2.80.
Wang W., Moe K.S. (2012) Lab Notes: Silicon-vacancy defect in HPHT-grown type IIb synthetic. *G&G*, Vol. 48, No. 4, pp. 304–305.
Watanabe K., Lawson S.C., Isoya J., Kanda H., Sato Y. (1997) Phosphorescence in high-pressure synthetic diamond. *Diamond and Related Materials*, Vol. 6, No. 1, pp. 99–106 http://dx.doi.org/10.1016/S0925-9635(96)00764-9.
Yelisseyev A., Kanda H. (2007) Optical centers related to 3d transition metals in diamond. *New Diamond and Frontier Carbon Technology*, Vol. 17, No. 3, pp. 127–178.
Zaitsev A.M. (2001) *Optical Properties of Diamond—A Data Handbook*. Springer-Verlag, Berlin.